Correlation effects in band ferromagnets as detected by energy- and angle-resolved spin-polarized photoemission: Ni(110)

Rolf Clauberg
Institut für Festkörperforschung der Kernforschungsanlage Jülich GmbH, D-5170 Jülich, West Germany
(Received 28 February 1983; revised manuscript received 6 May 1983)

Calculated spectra of photoemission from Ni(110) with the use of a single-step model of the photoemission process and with the inclusion of self-energy corrections within the t-matrix approximation are compared to the results of a recent energy-, angle-, and spin-resolved photoemission experiment with linearly polarized light ($h\nu=16.85$ eV). The power of this technique to study electronic structure of correlated, magnetic solids is for the first time fully exploited. Good agreement is found not only in peak positions, but also in relative intensities as well as line shapes. In addition, evidence is provided that surface relaxation is important for the full understanding of the electronic structure of this particular crystal surface.

I. INTRODUCTION

In a very recent spin-resolved photoemission experiment at high energy and angle resolution ($\Delta E\simeq 100$ meV, $\Delta\theta\simeq\pm 3°$) from Ni(110) using linearly polarized light[1] it was possible for the first time to obtain the complete information contained in photoemission spectra of ferromagnetic materials. The experimentally obtained spin-resolved energy-distribution curves (EDC) (separate EDC for majority- and minority-spin states) give the unambiguous separation of structures due to spin-split electronic states, which are hidden in spin-unresolved EDC. Furthermore, these EDC allow a direct comparison with quantitative photoemission calculations. This includes not only the comparison of peak positions but also the analysis of line shapes. Until now such a detailed analysis was hindered in spin-unresolved EDC of conventional photoemission by the rather small experimentally inferred exchange splitting of Ni ($\Delta=0.17$–0.33 eV). In most cases the superposition of the spin-split structures required fitting procedures even for the exact determination of the peak position.[2,3] The usual line shape assumed in such fitting procedures is a Lorentzian. In some cases an asymmetric Doniach-Sunjic line shape was used,[1,3] although it was introduced for the description of multielectron excitations in core-level spectra,[4] and consequently the physical meaning of its parameters is not clear in the analysis of band-structure effects.

In this work we will show that surprisingly good agreement in peak positions, relative intensities, and even line shapes can be achieved between the spin-resolved EDC recently obtained by Raue *et al.*[1] and our photoemission calculations, provided that self-energy corrections along the lines proposed by Liebsch[5,6] are included in the one-step model of the photoemission process.[7–10] It also turns out that surface relaxation of the open Ni(110) surface must be considered.

II. THE THEORETICAL MODEL

The model for the photoemission process is the same already successfully used in calculating the spin-polarization of the photoyield near threshold from Ni.[11] The sample is treated as a semi-infinite crystal with a generally constant spacing between the atomic layers parallel to the surface. The effects due to surface relaxation of the topmost layers will be discussed in Sec. III. The surface barrier is described by a truncated image potential. The influence of inelastic scattering processes of the excited electron is simulated by the inclusion of an imaginary part V_{0i} into the crystal potential. The energy-dependent values of V_{0i} are taken from the results of McRae and Caldwell for Ni(001) (Ref. 12) thereby neglecting small differences in V_{0i} due to different surface scattering processes. The self-energy of the hole state in the excited many-electron system is responsible for the narrowing of the d-band width, the decreased exchange splitting, and satellite structures.[13] These correlation effects make it necessary to go beyond the independent-particle model of self-consistent band-structure calculations. This is done by introducing the self-energy into the photoemission calculation by replacing the band energy $E_i(\vec{k})$ by the real part of the quasiparticle energy:

$$E_i(\vec{k})\rightarrow \mathrm{Re}e(\vec{k})=E_i(\vec{k})+\mathrm{Re}\Sigma(e),$$

where $\Sigma(e)$ is the complex self-energy. The well-known equation

$$I\propto(E_f-E_v)^{1/2}\sum_i |\langle\Psi_f|\vec{A}\cdot\vec{p}|\Psi_i\rangle|^2\delta(E_f-h\nu-E_i)$$

for the photoemission current in the one-particle approximation is thus changed to the equation

$$I\propto(E_f-E_v)^{1/2}\sum_i |\langle\Psi_f|\vec{A}\cdot\vec{p}|\Psi_i\rangle|^2 \times\delta(E_f-h\nu-\mathrm{Re}\Sigma(E_f-h\nu)-E_i)\ ,$$

where $\Psi_{i\,(f)}$ is the initial (final) state in photoemission, E_v the vacuum energy, $\vec{A}$ the vector potential of the exciting light, and $h\nu$ the photon energy. This corresponds to calculating the photoemission spectra with a so-called correlated band structure. Correlated band structures for Ni

have already been calculated by Davis and Feldkamp[14] and by Treglia *et al.*[15] for the directions ΓX and ΓL of the Brillouin zone. The present work is concerned with normal emission from Ni(110), i.e., the band structure along $\Gamma(\Sigma)K(S)X$. Bands allowed as initial states by dipole selection rules[16] are the Σ_4/S_4 bands ($|\vec{A}||[1\bar{1}0]$), the Σ_3/S_3 bands ($\vec{A}||[001]$), and the Σ_1/S_1 bands ($\vec{A}||[110]$). Besides a small p component, the Σ_4 band has the atomic symmetry $d_{x^2-y^2}$ in the cube coordinate system ($z||[001]$) along the whole direction ΓKX. This symmetry transforms as e_g states in a cubic crystal field. The Σ_3 band corresponds to a linear combination of the atomic symmetries d_{xz} and d_{yz} both belonging to the t_{2g} symmetry.

In the present work the self-energy is calculated in the t-matrix approximation of the low-density limit.[6] Liebsch[6] has shown that it is important to go beyond the low-density limit, particularly for a correct positioning of the satellite feature. Despite this fact, because of the present interest in states near E_F the calculations are restricted to the low-density limit with the Slater integrals in the calculation of the Coulomb matrix elements of the t matrix taken as $F^{(0)}=4$ eV, $F^{(2)}=8$ eV, and $F^{(4)}=0.6F^{(2)}$. These are the values leading to the exchange splittings $\Delta(e_g)=0.21$ eV, $\Delta(t_{2g})=0.37$ eV in Refs. 5 and 6. The first term in the t-matrix expansion gives the Hartree-Fock single-particle energy $\Sigma^{\mathrm{HF}}=-Un_{i,\sigma}$ (U equals the effective Coulomb energy, $n_{i,\sigma}$ equals the total number of the holes minus the number of holes with symmetry i and spin σ). Applying the self-energy correction to a self-consistent band-structure calculation means that at least the Hartree-Fock term must be subtracted from the self-energy $\Sigma(e)$, since it is already included. Band-structure calculations based on the density-functional method already implicitly include further correlations. Thus the energy to be subtracted from $\Sigma(e)$ is not exactly known. Since all the majority-spin bands are filled, $\Sigma_{\uparrow}^{\mathrm{HF}}$ is equal for bands of e_g and t_{2g} symmetry. Using this fact, we assume an equal energy of -1.27 eV to be subtracted from $\Sigma(e)$ for both e_g and t_{2g} states and apply the corrected self-energy to the majority-spin band structure of Moruzzi *et al.*[17] This correction is chosen to adjust the $X_5^{\uparrow}$ point to 0.1 eV below the Fermi energy to reach agreement with earlier experimental observations.[1,2] This procedure can be compared with the adjustment of the origin of energy in the work of Davis and Feldkamp[14] or the redetermination of the Fermi energy by Treglia *et al.*[15] Then a rigid exchange splitting of 0.21 eV for the Σ_4/S_4 band and of 0.37 eV for the Σ_3/S_3 band is used instead of using uncertain values to correct $\Sigma_{\downarrow}(e_g)$ and $\Sigma_{\downarrow}(t_{2g})$.

III. RESULTS AND DISCUSSION

For Ne I radiation ($h\nu=16.5$ eV) the normal photoemission from Ni(110) is mainly due to emission from the region near the X point into a final-state band gap between the $X_{5'}$ and the X_3 point. The corresponding correlated band structure from K to X is given in Fig. 1 (where we did not include the S_2 band, which is not an allowed initial state for normal emission).

Figure 2 shows the experimentally obtained spin-resolved EDC (Ref. 1) and the results of our photoemission calculations. According to the fact that direct transitions occur only from the X points into evanescent final states (the complex continuation of the S_1 final-state band between the $X_{5'}$ and the X_3 point), the mean escape depth is about $8a_0$ (a_0 is the Bohr radius) or about 3.5 atomic layers parallel to the (110) surface. This should be compared to the mean free path of about $25a_0$, which is the mean escape depth for propagating final states. The resulting relaxation of $k_{\perp}$ conservation gives rise to spectra with quite broad structures, even without the inclusion of a lifetime broadening of the initial states (compare Fig. 2). The spectra with S_3 initial states show an extraordinarily large width. This results from the relatively small distance to the X point even for binding energies 0.4 eV below X_5, giving still considerable weight to indirect transitions from the S_3 band into the complex continuation of the S_1 final-state band. The asymmetric line shapes in Fig. 2 are a direct consequence of these indirect transitions, since the band edges at $X_2^{\downarrow\uparrow}(X_5^{\uparrow})$ give upper energy limits to the spectra. In this context we mention that interesting effects can be expected when changing the surface sensitivity by means of tunable, polarized light from a storage ring.

Besides the reduced $k_{\perp}$ conservation there is a second ef-

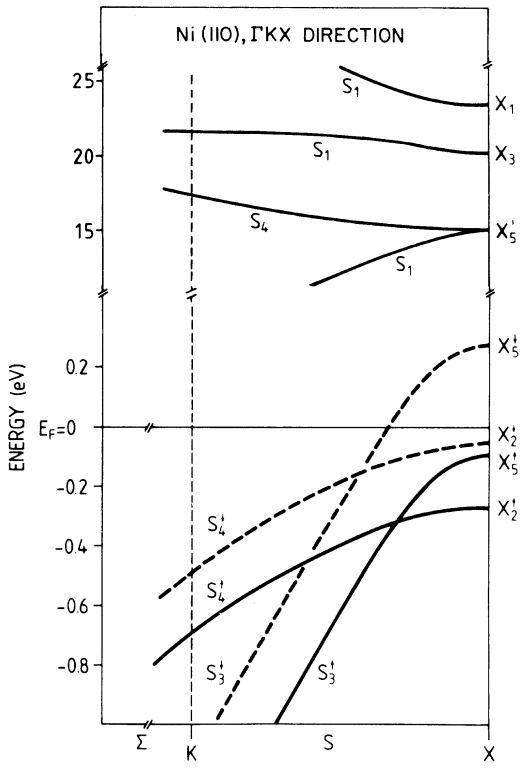

FIG. 1. One-dimensional ferromagnetic band structure along the $K(S)X$ direction including self-energy corrections for the initial states. Only initial states are shown which are allowed in normal emission. Note the different energy scale for the final states.

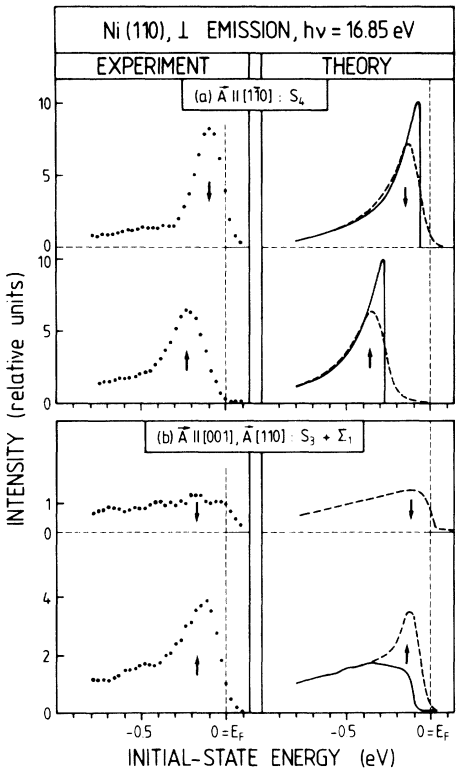

FIG. 2. Experimental and calculated spin-resolved energy-distribution curves for normal emission from Ni(110) (a) for the electric field vector in the [1$\bar{1}$0] direction, and (b) for the electric field vector mainly in the [001] direction with a small component in the [110] direction. The dashed curves in the theory include the lifetime broadening of the hole state and the experimental resolution (see text). The proportionality factor between the experimental count rates and the units in the calculations is chosen to give equal peak heights for the measured and calculated $S_4^{\uparrow}$ spectrum. In the majority-spin spectrum of (b), the dashed line corresponds to an incoherent addition of contributions to the transition matrix element (see text) and it includes the experimental resolution.

fect to be considered which occurs in a perfect semi-infinite crystal and reduces the emission intensity from regions near high-symmetry points (except the K point) in the calculated spectra. This is a destructive interference in the initial state of the semi-infinite crystal which can be understood as follows. The initial state is given as a linear combination of complex Bloch waves.[7] Considering as a first approximation only the Bloch wave propagating to the surface and the reflected one propagating into the solid, one finds for the layer density of states

$$\rho^{(n)}=4\rho^{\infty}(E,\vec{k}_{||})\sin^2(\vec{k}\cdot\vec{d}n)\ ,$$

where n is the layer index ($n=1$ for the surface layer), $\vec{k}$ the Bloch vector, and $\vec{d}$ the lattice vector pointing from one atom to the neighbor atom in the next atomic layer. ρ^{∞} is the density of states of the corresponding single Bloch state. The sine term leads to a strong decrease of $\rho^{(n)}$ if $2n\vec{k}$ comes close to a reciprocal-lattice vector. This is the case for every n at all high-symmetry points except the K point. In the calculated $S_3^{\uparrow}$ spectra this destructive interference nearly destroys the peak (see bottom right of Fig. 2), in obvious disagreement with the experiment.

In the experiment there are two effects which can reestablish this peak. Firstly, the Ni(110) surface is relaxed, i.e., the top-layer distance is smaller by about 5% than the bulk layer spacing.[18] This softens the interference condition. To approximate this situation we have calculated an $S_3^{\uparrow}$ spectrum, where the different contributions to the transition matrix element are added incoherently thereby avoiding the destructive interference condition. This spectrum agrees fairly well with the experiment [Figs. 2(b) and 3]. Certainly, adding all layer contributions incoherently tends to overestimate the softening of the interference condition and consequently the intensity of the reestablished peak. On the other hand, the approximation is expected to be quite reasonable since the interference effect is most important for the first layer ($n=1$), where the relaxation effects show up predominantly. This is valid especially in the present experimental situation where the very short mean escape depth of the photoelectrons gives strong weight to the emission from the very first layers. Thus a structure which exists in the emission from the first two layers should also play a dominant role in the total emission spectrum.

The S_4 spectra, on the other hand, are nearly unaffected

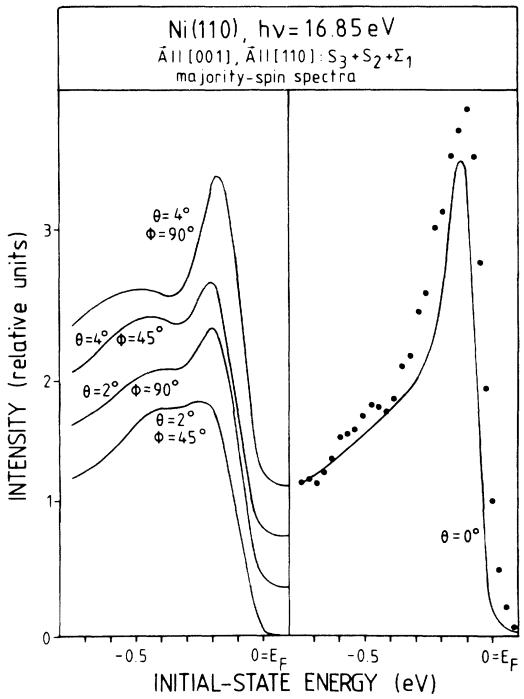

FIG. 3. Comparison of some selected off-normal emission spectra ($\vec{A}||[001]$, $\vec{A}||[110]$, majority spin) with the incoherently added spectrum for normal emission ($\theta=0°$) and with the experimental data (closed circles). All spectra include the experimental resolution. The proportionality factor between the experimental count rates and the units in the calculations is the same as in Fig. 2. The off-normal spectra are displaced for better visibility.

by this interference effect since the corresponding $\vec{k}$ vectors do not match with the interference condition already for initial states at slightly higher binding energies than X_2. This is so although there is no emission intensity directly from the X_2 point.

The second important effect giving spectral weight for states near E_F in the case of the $S_3^{\uparrow}$ spectrum is due to the off-normal emission contribution which is connected with the finite acceptance cone of the experiment. This results in S_2 band emission to the S_3 spectra according to the mixing of S_3 symmetry into the S_2 band near the X_5 point (the S_2 and the S_3 band are degenerate at the X_5 point) and of S_4 symmetry into the S_1 final-state band near $X_{5'}$ (the S_1 and an S_4 band are degenerate at the $X_{5'}$ point; see Fig. 1). The symmetry change in the final-state band is found to be most important. The contributions to the S_4 spectra are negligible. Spectra have been calculated for polar angles up to 4°, which already exceeds the experimental angular acceptance cone of Ref. 1. The strongest effect is seen for $\vec{A}||[001]$, a polar angle of $\theta=4°$, and an azimuthal angle of 90° with respect to [001] for electron take-off (Fig. 3). The spectrum already shows a remarkable peak at about 0.17 eV below E_F, but by comparison with the experimental spectrum (in Fig. 3 displayed in the same units as in Fig. 2), one finds that the off-normal contribution is still much too small. If one takes the small structure around -0.5 eV in the experimental data as significant, one could connect this with the shoulder in the calculated off-normal emission spectra. Thus this structure and the larger width of the prominent peak in the experimental spectrum as compared to the incoherently added normal emission spectrum (Fig. 3) may be a result of off-normal emission contributions. We expect, however, that off-normal emission alone is not able to explain the experimental data, because of the integration over the full experimental acceptance cone ($\Delta\theta=\pm 3°$, Ref. 1). By implying that misalignment effects in the experiment are considerably smaller than the acceptance cone, we therefore conclude that the relaxation effect is likely to be the dominating one. This again demonstrates the importance of surface relaxation on the electronic properties of the Ni(110) surface. We therefore deduce that improved angular resolution can help to quantitatively establish the different effects.

The S_3 spectra contain a small contribution from Σ_1 band emission according to the component $\vec{A}||[110]$, because of the incidence angle of the light (30°).[1] However, the calculations give emission intensities for the Σ_1 band which are smaller by at least 1 order of magnitude than the intensity of the S_3 band in the whole energy range of the experiment. This emission is contained in the calculated spectra and accounts for the small wiggles between 0.3 and 0.6 eV in the unbroadened $(S_3^{\uparrow}+\Sigma_1^{\uparrow})$ spectrum.

The relative intensities of the S_4 and S_3 emission spectra calculated as described above are already in fairly good agreement with the experimental results. In addition, the S_4 spectra have been convoluted firstly with a Lorentzian of γ (halfwidth at half maximum) $=\mathrm{Im}\Sigma(e)$ $=0.004(0.015)$ eV at the minority- (majority-) spin peak position to account for the lifetime of the hole state, and secondly with a Gaussian of γ [full width at half maximum (FWHM)] $=0.100$ eV to include the experimental resolution. As can be seen from Fig. 2 not only is the general line shape of the experimental spectra reproduced, but also the absolute widths of the calculated spectra (FWHM$=0.26$ eV for $S_4^{\uparrow}$ and 0.23 eV for $S_4^{\downarrow}$) and the intensity ratio (equal to 1.12) are in acceptable agreement with the experimental widths of 0.26 and 0.20 eV, respectively, and with the intensity ratio of 1.20. We believe that a better agreement can only be expected with an improved self-energy correction. We also mention that the convolutions of the asymmetrical spectra have shifted the peak positions slightly to higher binding energies. Consequently, referring to the experimental spectra, the $X_2^{\downarrow\uparrow}$ and $X_5^{\uparrow}$ points should be expected to be located nearer to E_F than given in Fig. 1. Even an $X_2^{\downarrow}$ point energy coinciding with the Fermi energy is still compatible with the experimental data. Similar observations have recently been made for Fe(001).[19]

IV. CONCLUSION

In summary, it was shown that photoemission calculations with the use of a single-step model of the photoemission process and with the inclusion of self-energy corrections provide quantitative agreement in peak positions, relative intensities, and line shapes of experimentally obtained spin- and angle-resolved energy-distribution curves of Ni(110) as a model system for a correlated magnetic metal, thus allowing an accurate determination of critical point energies and exchange splittings in Ni near X. We have also shown that surface relaxation is important for fully understanding the Ni(110) crystal surface. Finally, because of the excellent agreement between theory and experiment, we believe that an inelastic spin-polarized background, including spin flip,[19–21] plays no important role for this system in the energy range near E_F.

The calculations will provide a basis for studying temperature-dependent effects on the magnetic (exchange) splitting and their experimental observation. This program is in progress in our laboratory as well as the German storage ring Berliner Elektronenspeicherring-Gesellschaft für Synchrotronstrahlung mbH (BESSY) in Berlin.

ACKNOWLEDGMENTS

I would like to thank A. Liebsch for helpful discussions and providing numerical data on the Ni electronic structure and W. Gudat for helpful discussions. This work was performed within the subject of a research project on correlation effects and spin polarization in magnetic metals. I am grateful to M. Campagna for his suggestions and support to this project.

[1]R. Raue, H. Hopster, and R. Clauberg, Phys. Rev. Lett. 50, 1623 (1983).
[2]P. Heimann, F. J. Himpsel, and D. E. Eastman, Solid State Commun. 39, 219 (1981).
[3]C. J. Maetz, U. Gerhardt, E. Dietz, A. Ziegler, and R. J. Jelitto, Phys. Rev. Lett. 48, 1686 (1982).
[4]S. Doniach and M. Sunjic, J. Phys. C 3, 285 (1970).
[5]A. Liebsch, Phys. Rev. Lett. 43, 1431 (1979).
[6]A. Liebsch, Phys. Rev. B 23, 5203 (1981).
[7]A. Liebsch, in *Electron and Ion Spectroscopy of Solids,* edited by L. Fiermans, J. Vennik, and W. Dekeyser (Plenum, New York, 1978).
[8]P. J. Feibelman and D. E. Eastman, Phys. Rev. B 10, 4932 (1974).
[9]D. Spanjaard, D. W. Jepsen, and P. M. Marcus, Phys. Rev. B 15, 1728 (1977).
[10]D. W. Jepsen, F. J. Himpsel, and D. E. Eastman, Phys. Rev. B 26, 4039 (1982).
[11]R. Clauberg, Phys. Rev. B 27, 4644 (1983).
[12]G. McRae and C. W. Caldwell, Surf. Sci. 57, 766 (1976).
[13]A. Liebsch, in *Festkörperprobleme,* Vol. XIX of *Advances in Solid State Physics,* edited by J. Treusch (Vieweg, Braunschweig, 1979), p. 209.
[14]L. C. Davis and L. A. Feldkamp, Solid State Commun. 34, 141 (1980).
[15]G. Treglia, F. Ducastelle, and D. Spanjaard, J. Phys. (Paris) 43, 341 (1982).
[16]J. Hermanson, Solid State Commun. 22, 9 (1977).
[17]V. L. Moruzzi, J. F. Janak, and A. R. Williams, *Calculated Electronic Properties of Metals* (Pergamon, New York, 1978).
[18]J. E. Demuth, P. M. Marcus, and D. W. Jepsen, Phys. Rev. B 11, 1460 (1975).
[19]R. Feder, W. Gudat, E. Kisker, A. Rodriguez, and K. Schröder, Solid State Commun. (in press).
[20]H. Hopster, R. Raue, E. Kisker, G. Güntherodt, and M. Campagna, Phys. Rev. Lett. 50, 70 (1983).
[21]E. Kisker, W. Gudat, and K. Schröder, Solid State Commun. 44, 591 (1982).